Plant Soil (2009) 318:243–255
DOI 10.1007/s11104-008-9834-7

REGULAR ARTICLE

# Neutron radiography as a tool for revealing root development in soil: capabilities and limitations

**Ahmad B. Moradi · Héctor M. Conesa · Brett Robinson · Eberhard Lehmann · Guido Kuehne · Anders Kaestner · Sascha Oswald · Rainer Schulin**

Received: 8 August 2008 / Accepted: 10 November 2008 / Published online: 9 December 2008


**Abstract** Neutron Radiography (NR) is a valuable non-invasive tool to study in situ root development in soil. However, there is a lacuna of quantitative information on its capabilities and limitations. We combined neutron radiography with image analysis techniques to quantify the neutron absorption coefficients ($\Sigma$) of various root-growth media for a range of water contents ($\theta$) in the presence and absence of plant roots with various rooting systems. Plants were grown in aluminium containers (170×150×12 mm) and were imaged using NR, as well as X-Ray radiography and an optical scanner. Sandy soil was the best medium for NR because it supported plant growth at $\theta$ that gave a good contrast for root visualisation. After correction for neutron scattering, we obtained a linear correlation between $\Sigma$ and soil $\theta$. The minimum detectable root thickness in neutron radiographs was found to be 0.2 mm in these containers. Combining NR with X-Ray radiography could provide information on soil structure in addition to revealing root structure and development.

**Keywords** Neutron radiography · Neutron attenuation coefficient · Neutron scattering · Plant roots · Soil water content · X-ray radiography

Responsible Editor: Hans Lambers.

A. B. Moradi (✉) · H. M. Conesa · B. Robinson · R. Schulin
Institute of Terrestrial Ecosystems, Soil Protection group, ETH Zurich,
CHN F28.2, Universitaetstrasse 16,
CH-8092 Zurich, Switzerland
e-mail: ahmad.moradi@env.ethz.ch
URL: http://www.ito.ethz.ch/soilprot/

E. Lehmann · G. Kuehne · A. Kaestner
Paul Scherrer Institut,
Villigen, Switzerland

S. Oswald
Helmholtz Centre for Environmental Research - UFZ,
Leipzig, Germany

## Introduction

Neutron Radiography (NR) is one of the few non-destructive techniques available to image living plant roots in situ (Menon et al. 2007). Roots grow in a heterogeneous, porous, semi-compressible medium compound of solid, liquid and gaseous phases, known as soil. It is difficult to observe tightly enmeshed roots in an opaque soil matrix without disturbance. Better understanding of root behaviour in heterogeneous soil, requires efficient non-invasive techniques to analyze root and soil structure in situ (Fitz et al. 2005; Pierret et al. 2005; Nakaji et al. 2008; Pierret 2008).

Current non-invasive and non-destructive methods for studying roots include minirhizotrons which are

transparent plastic tubes inserted into the ground to view the roots using a camera (Kuchenbuch and Ingram 2002), magnetic resonance imaging (Bottomley et al. 1993; Doussan et al. 2003; Heyes and Clark 2003), neutron radiography and tomography (Willatt et al. 1978; Willatt and Struss 1979; Bois and Couchat 1983; Nakanishi et al. 2005; Menon et al. 2007; Oswald et al. 2008; Tumlinson et al. 2008) as well as X-Ray imaging and tomography (Moran et al. 2000; Naftel et al. 2001; Gregory et al. 2003; Pierret et al. 2003b). Root observation using minirhizotrons is non-destructive. However, they have an invasive component that may perturb root development and water flux (Majdi 1996). Ferromagnetic materials hinder magnetic resonance imaging (Hall et al. 1997), thus limiting this technique to carefully selected media such as pre-treated sand and soil, agar, and glass beads. NR provides images similar to X-Ray radiography. Neutrons interact with the nuclei of atoms while X-Rays interact with electrons. Whereas X-Ray attenuation depends on element's atomic number $Z$, the neutron attenuation coefficient is independent of $Z$ and only a few elements such as hydrogen strongly attenuate neutrons. Therefore, H-rich, organic materials and water are clearly visible in neutron radiographs, while many soil components and structural materials such as Si, Ca and Al are nearly transparent. This permits in situ investigations of specimens housed in various types of experimental apparatus. Such housings often impair or prevent X-Ray imaging because of their high X-Ray cross sections. However the neutron cross section of these elements is moderately low, allowing the neutrons to pass through undisturbed.

NR is a valuable tool for studying root behaviour in soil since the difference in gravimetric water content ($\theta$) of roots and the surrounding soil provides enough contrast to visualize the roots. Nakanishi et al. (2005) showed how soil $\theta$ changes along a vertical distance from the root surface using thermal neutron beam analysis. Microscopic movement of water around the roots of soybean seedlings was studied by Furukawa et al. (1999). Menon et al. (2007) visualized the root growth of lupin plants over a period of 3 weeks and revealed how heterogeneous soil can affect root growth. Fine roots (<2 mm) are particularly important for the uptake of water and nutrient by plants (Sutton and Tinus 1983; Waisel et al. 2002). While it is widely recognized that the total length of the fine roots is generally larger than that of the coarse roots of a plant, it is also acknowledged that the amount of fine roots is often underestimated because of the lack of reliable measurement techniques, their small size and near transparency (Vogt et al. 1998; Costa et al. 2001; Pierret et al. 2003a). Root visibility in NR is proportional to root thickness and inversely proportional to soil moisture content (Furukawa et al. 1999; Nakanishi et al. 2003, 2005; Matsushima et al. 2005; Menon et al. 2007). These authors used either thin containers (as thin as 2 mm) or artificial plant growth media (quartz sand or silt). There is a lacuna of information on the performance of NR in other systems, for example with topsoils, and more realistic growing containers. The effects of root thickness, soil type and the water content of the surrounding soil on the contrast between soil and roots in NR images has not been quantified and the capability of NR has not yet been evaluated in visualizing fine roots with various thickness in various soil types and water contents.

The quantitative analysis of a neutron radiograph requires corrections for interactions between neutron beam and the sample other than adsorption, which can be significant. These types of interactions can be coherent, incoherent, elastic an inelastic scattering. Calibrating of the $\theta$ against neutron transmission usually may not give a satisfactory result, especially at higher $\theta$ where transmission decreases and multiple neutron scattering becomes important leading to a considerable deviation from the exponential law of attenuation (Hassanein 2006). While neutron scattering is used to measure various properties of materials (Bailey 2003), it needs to be corrected for studying water and hydrogen rich organic materials, such as roots, in soil.

We aimed to assess the capabilities and limitations of NR combined with image analysis tools for studying non-destructively root development in soil with particular attention to the quantitative effects of neutron scattering, soil type, soil $\theta$ and root thickness on the root visibility in soil. Specifically, we sought to quantify the effects of soil type, soil moisture, and container dimensions and size on the ability to visualise roots and determine the detection limits for NR under realistic conditions for plant growth. Furthermore, we aimed to develop NR as a tool to quantify the water content of soil in the rhizosphere.

## Materials and methods

### Neutron and X-Ray radiography systems

The Beer-Lambert law describes the attenuation of both neutron and X-Ray radiation (Kasperl and Vontobel 2005), assuming that the neutron detector records only the uncollided flux component and that the neutrons are mono-energetic or have a small wavelength bandwidth:

$$I = I_0.e^{-\Sigma.d} \quad (1)$$

where $I$ is the detected neutron flux ($cm^{-2}\ s^{-1}$) after an incident neutron flux, $I_0$, passes through material of thickness $d$ (cm) with a neutron attenuation coefficient of $\Sigma$ ($cm^{-1}$), which is a bulk physical property of the material. The material may be crystalline, polymorphic, or, as in our case, a porous media.

The experiments were performed at the neutron and X-Ray radiography facilities at Paul Scherrer Institut (PSI), Villigen, Switzerland. Both neutron imaging facilities at PSI; NEUTRA for thermal neutrons (Lehmann et al. 1999), and ICON for imaging with cold neutrons (Kuhne et al. 2005), consist of the neutron source (the spallation neutron source SINQ), a special collimator, and a two-dimensional image detector. For a thermal spectrum, the moderator is kept at about room temperature (~300 K), which yields neutron energies of around 25 meV and velocities of around 2200 m/s. For a cold spectrum, liquid deuterium is used as an additional moderator at around 25° K, yielding neutron energies of around 5.7 meV and velocities of about 1000 m/s. The collimator is a beam-forming assembly that determines the geometric properties of the beam and contains filters that reduce the intensity of accompanying gamma rays. The image resolution depends on the collimator geometry and is expressed by the collimation ratio $L/D$, where $L$ is the collimator length and $D$ is the diameter of the inlet aperture of the collimator on the side facing the source. In our study, a neutron flux of $4.2\times10^6$ $cm^{-2}\ s^{-1}$ with a mean energy of 25 meV and a collimation ratio of $L/D$= 550, was used for NEUTRA while for ICON a neutron flux of $2.8\times10^6$ $cm^{-2}\ s^{-1}$, a mean energy of 5.7 meV, and a collimation ratio of $L/D$=605. The beam was transmitted through the sample and an area position-sensitive detector recorded the resulting image, which is integrated in the beam direction over the thickness, d. This detector records a two-dimensional image that is a projection of the object on the detector plane. We used a CCD camera detector with an array of 1024×1024 pixels in conjunction with a neutron-sensitive $^6$Li based scintillator screen (Applied scintillation technologies, UK), giving a resolution of 110–170 μm in the digital images.

The X-Ray radiography facility at PSI consists of an X-Ray tube with a maximal voltage of 320 kV. Using the focal spot at the tungsten target of about 3 mm, which corresponds to arrangement of the tube just in front of the outer collimator close to the target block wall, we obtained about the same $L/D$ ratio as with the neutron beam. A scintillator screen made of Gadolinium-oxy-sulfide (Gadox) was used for X-Ray imaging.

### Materials testing

We chose a variety of materials that could be potentially used as root growth media (Table 1). The materials were air-dried and packed into the plant growth containers and were imaged the same way as the plant roots. We used containers with inner dimensions of 0.17×0.15×0.012 m. The containers were made of aluminium because of its low neutron attenuation and therefore high transparency.

### Calibration for soil water content

The NR image is a projection of the object (in our case a container with a thickness of 12 mm) in the direction of the container thickness. Thus both soil water and water residing in the roots contribute to the neutron attenuation coefficients calculated pixel-wise in each image. The contrast in the NR images comes from difference in water content of the roots and the surrounding soil. Calibrating neutron attenuation coefficients against soil water is needed to calculate the contribution of root water to the $\Sigma$, knowing the root diameter. To calibrate neutron transmission and $\Sigma$ against soil $\theta$, three containers were filled with the sandy soil (Table 1) in the same way as described above. The soils were saturated with water, then left to dry for 2 weeks at room temperature by opening one side of the container. The containers were imaged seven times during the drying period. Before each imaging, the total water content of the soil was measured gravimetrically.

**Table 1** Physical properties of the plant growth media used for neutron radiography

| | Particle size (mm) | Bulk density (g $cm^{-3}$) | Porosity (% v/v) | Water holding capacity at 100 kPa ($cm^3/cm^{-3}$) | Provenience |
|---|---|---|---|---|---|
| Perlite | <2 | 0.125 | 97 | 0.91 | Samen Mauser, Switzerland |
| Porous glass beads | 1.5 – 2.5 | 0.49 | 71 | 0.16 | Schott, Germany |
| Mine tailing soil | <2 | 1.4 | 35 | 0.08 | Southeast, Spain |
| Loamy soil | <2 | 1.2 | 49 | 0.17 | Mattenweg, Switzerland |
| Organic soil | <2 | 0.58 | 88 | 0.09 | Migros, Switzerland |
| Sandy soil | <2 | 1.3 | 36 | 0.09 | Eiken, Switzerland |
| Fine quartz sand | 0.1–0.7 | 1.5 | 19 | 0.01 | Carlo, Switzerland |
| Coarse quartz sand | 0.7–1.5 | 1.45 | 26 | 0.01 | Carlo, Switzerland |

## Plant growth

Three plant species, with three different rooting systems were selected for this study; garden tomato (*Lycopersicon esculentum* Mill.) with a fibrous root system of fine roots, chickpea *(Cicer arietinum* L.*)* with strong tap root system and *Berkheya coddii* Roessl with a fibrous root system of both fine and coarse roots. We filled 12 containers with the sandy loam described in Table 1. There were four treatments, each with three replicates: the three aforementioned plants and an unplanted treatment. The average bulk density of the packed soil was 1.3 g $cm^{-3}$. The seeds of the plants were sown directly onto the soil surface at the centre of the containers except for *Berkheya coddii*, where seedlings were transplanted into the containers. The plants were grown for 7 weeks before the imaging in a controlled environment chamber at 16–19°C and a daily photoperiod of 16 h generated by fluorescent lighting (0.4–0.6 lumen $cm^{-3}$). Plants were irrigated with Hoagland's nutrient solution (Hoagland and Arnon 1938) to maintain soil $\theta$ of around 20%. Irrigation was stopped 3 days before imaging. Neutron and X-Ray radiographs were taken on the same day. After imaging, we opened one side of the containers and scanned the soil surface using a conventional photo scanner with a pixel array of 2250×2250. Soil in the containers was subdivided into sections. Each section was weighted and the roots were carefully separated from the soil. The dry mass of the roots as well as the moisture content of the soil in each section were determined by weighing.

## Imaging procedure

All containers were imaged in exactly the same position using an automated positioning table in front of the beam line with a distance of 10 cm from the scintillator plane in the ICON setup and 15 cm in the NEUTRA and X-Ray setups (Fig. 1). We used exposure times of 45, 15 and 10 s for ICON, NEUTRA and X-Ray images respectively. These exposure times gave the best signal to noise ratio and therefore the best contrast between the roots and the soil. X-Ray images used a voltage of 120 kV at 10 mA. To correct for spatial variations in beam intensity, we collected open beam images and dark current images. The field of view was 19×17 cm which left a margin (area without sample) of 1 cm. This was used to normalise the images and to correct for any fluctuations in beam intensity.

## Image analysis

The transmission images were first corrected for beam variation and camera noise using a flat field correction. The corrected image ($I'$) was calculated as:

$$I' = f_{OB} \cdot \frac{I_{raw}(x,y)/I_{dark}(x,y)}{I_{OB}(x,y)/I_{dark}(x,y)} \quad (2)$$

where $I_{raw}(x,y)$ is the raw image, $I_{dark}(x,y)$ is the image with neither beam nor sample, $I_{OB}(x,y)$ is the open beam image containing the spatial variation of the beam without the sample, and $f_{OB}$ is a scaling factor. The calculations were performed pixelwise and $x$ and $y$ are the coordinates. The value for $f_{OB}$ was

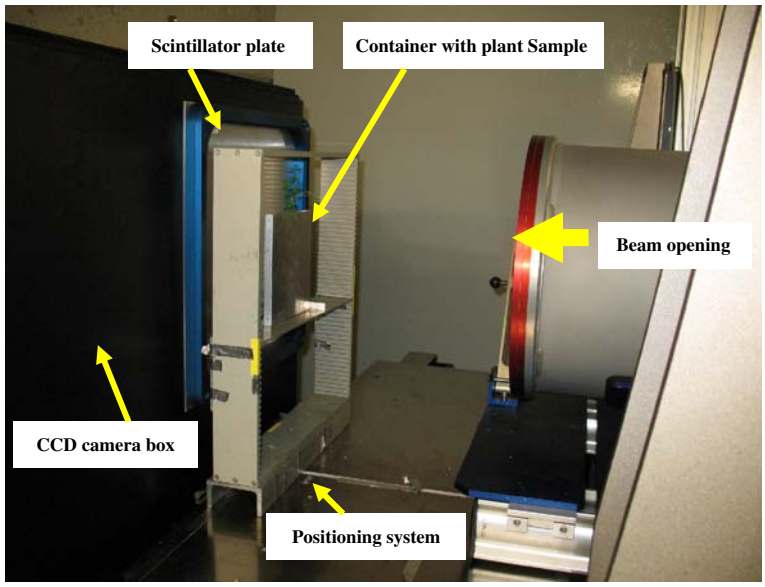


**Fig. 1** The cold-neutron imaging set-up (ICON) at PSI

chosen so that the mean transmission in the regions of the image without the sample was 1. Based on Eq. 1 the negative logarithm of the corrected image, *I'(x,y)*, yields the attenuation coefficient $\Sigma$ *(x,y)* of the material summed over the sample thickness *d*. The corrected transmission image shows a consistent contrast between different substances in the image. For example, roots appear darker than the surrounding soil because of their lower transmission due to the higher $\Sigma$.

The distinction between absorbed and scattered neutrons is critical for quantitative NR analysis. Some scattered neutrons collide with the detector plate and thus cause deviations from the exponential law of attenuation (Eq. 1). The scattering component increases image intensity and may lead to an underestimation of the neutron attenuation or density of the materials. Surrounding objects, such as the camera box or neutron shielding can scatter neutrons into the detector. Since these neutrons would have otherwise missed the objective, the scattering causes an extra intensity. Hydrogen, the main neutron-opaque component of the root-soil system, scatters a relatively high number of neutrons. Further deviations from the exponential law of attenuation are due to beam hardening and the energy dependency of the detector efficiency. We used the Quantitative Neutron Imaging algorithm (QNI) to correct for scattering and beam hardening (Hassanein et al. 2005). The correction is based on the iterative reconstruction of the measured image by overlapping point scattered functions calculated by means of Monte-Carlo simulation (Hassanein 2006).

For samples made of different substances; such as an aluminium container with soil, roots, and water, the total $\Sigma$ is then sum of the individual components:

$$\sum_{total}(x,y) = \left(\sum_{Soil}(x,y) + \sum_{Aluminium}(x,y) + \sum_{Water}(x,y)\right) = \frac{1n\left(\frac{I_0}{I}\right)}{d} \quad (3)$$

The component accounting for the water in the system, $\Sigma_{water}$, comprises from both soil and root water. If the root thickness and the soil water content are known, the total $\Sigma$ of water can be calculated from the water residing in the soil and water in the roots:

$$\sum_{Water}.d = \left(\sum_{rootwater}.x\right) + \left(\sum_{soilwater}.(d-x)\right) \quad (4)$$

where *d* is the container thickness filled with soil and *x* is the root thickness.

We used the same method as Menon et al. (2007) for detecting root thickness and segmentation. All other calculations above apart from the neutron scattering correction were carried out using Matlab.

## Results

### The analysis of a neutron radiograph

Figure 2 shows a NR image of a root system grown in an aluminium container filled with soil together with the transmission values along a cross-section through the image. There was a clear contrast between the soil and the roots, although the signal from the soil was heterogeneous due to the differences in the soil moisture content and the soil-filling patterns. Normalizing the image set a mean transmission value of 1 for the open beam area, while the sample area had different transmission based on its $\Sigma$. The aluminium frame of the container with a thickness of 16 mm absorbed only 5% of the incident neutrons resulting in a transmission value of 0.95. The aluminium sidewalls of the container had a thickness of 3 mm and therefore a mean transmission value of 0.99. The contrast between the roots and the soil was due to their different $\theta$.

### The effect of plant-growth medium on root contrast

Figure 3 shows the cold-neutron $\Sigma$ value of tested plant-growth media. The dry porous glass beads (Schott, Germany) used in this study had the highest $\Sigma$ (1.44 $cm^{-1}$) and thus the lowest transmittance. This is because the glass beads contained high concentrations of boron, which strongly absorbs neutrons. Perlite gave the lowest $\Sigma$ (0.07 $cm^{-1}$), which can be attributed to its low bulk density. In the sand and sandy-soils, the neutron absorption increased in proportion to the concentration of fine materials, in particular clay. The $\Sigma$ increased in the sequence sand < sandy soil < loamy soil. The high attenuation of

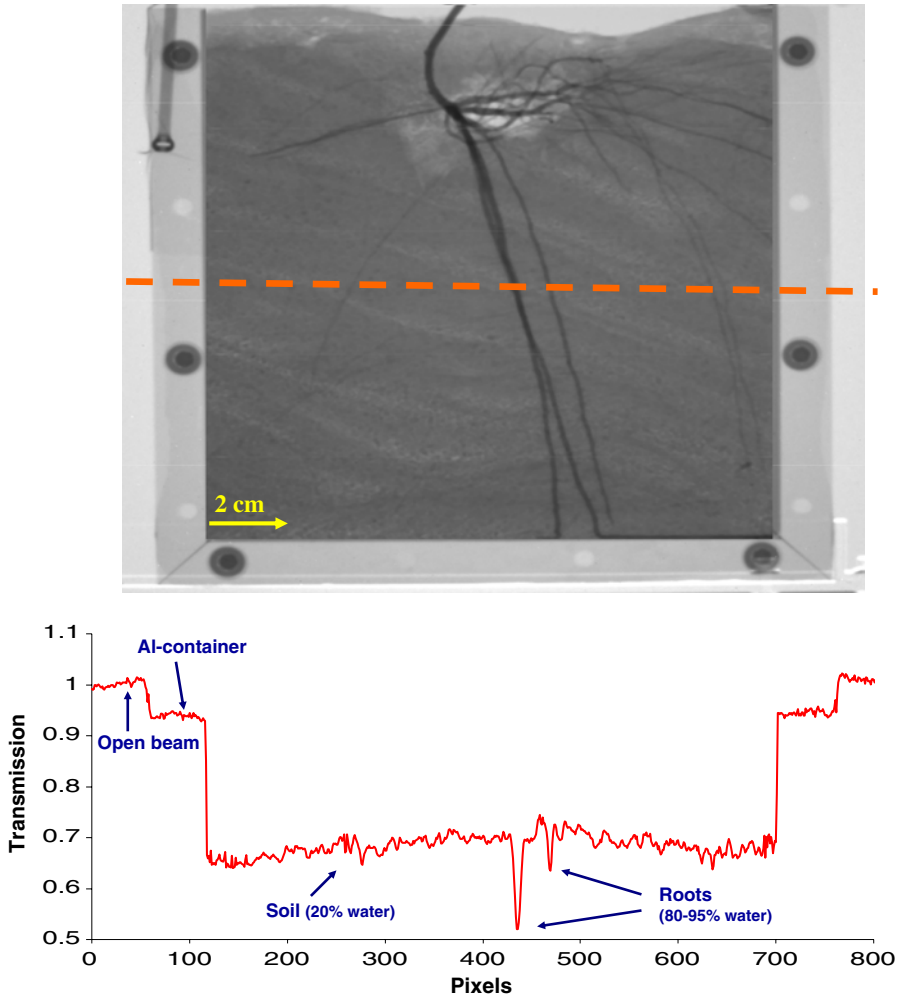


**Fig. 2** Neutron radiograph of *Berkheya coddii* roots in an aluminium container filled with soil. The graph shows the transmission values of the pixels along the cross-section in the image

neutrons in the organic soil and the mine tailings can be attributed to their high concentrations in hydrogen and iron, respectively.

For most plants, the optimal soil moisture for growth is between field capacity (ca −33 kPa) and a water potential of −100 kPa (Allen et al. 1998). Reducing the soil $\theta$ improves contrast. Therefore, the optimal soil moisture for imaging roots by NR is at a soil water potential at the dry end of this range (−100 kPa). Plotting the $\Sigma$ of the plant growth media containing their corresponding $\theta$ at −100 kPa changed the trend completely (Fig. 3). While dry perlite had the lowest $\Sigma$, perlite had the highest $\theta$ (Table 1) and therefore also the highest $\Sigma$ at −100 kPa.

## Relationship between the $\Sigma$ and $\theta$

Figure 4a shows the cold-neutron $\Sigma$ of water in soil over a range of soil $\theta$. The relationship between the uncorrected $\Sigma$ became non-linear at soil $\theta$ above 0.1 resulting in a loss of sensitivity. There was a 46% deviation from linearity at a soil $\theta$ of 0.07 and an 80% deviation at a soil $\theta$ of 0.25. Correcting for neutron scattering, the neutron attenuation coefficient of soil water showed a linear relationship with the water content of the soil. This result was in good agreement with the theoretical values for the neutron attenuation coefficient of a water layer calculated from the exponential law of attenuation. A similar relationship was observed between the thermal-neutron $\Sigma$ and soil $\theta$, except that the change of $\Sigma$ over soil $\theta$ and the slope of the curve were smaller than those obtained using cold neutrons (data not shown). The thermal-neutrons curve thus displayed lower sensitivity than the one for cold neutrons. Therefore we used the cold-neutron calibration curve for the rest of the analysis.

The total cold-neutron $\Sigma$ (sum of soil and soil water $\Sigma$) followed the same trend as the neutron $\Sigma$ of water (Fig. 4b). The intercept was equal to the $\Sigma$ of the dry soil (0.33 $cm^{-1}$). The relationship between the scattering-corrected total neutron $\Sigma$ and soil $\theta$ was linear ($R^2$=0.966, Pearson confidence level >0.99).

## Root detection

The ease of root detection in neutron radiographs increases in proportion to their $\theta$ and thickness. Coarser roots absorb or scatter more neutrons passing through the sample than fine roots. Therefore they create a better contrast with the surrounding soil. Figure 5a shows the contrast between roots and the surrounding soil (difference in $\Sigma$) for different root diameters over a range of soil $\theta$. These calculations are based on extracted attenuation coefficient of soil in different water contents and equations 3 and 4 assuming a container thickness of 12 mm and an average root $\theta$ of 85%. Contrast increased with increasing root diameter and also with decreasing soil water content for each root diameter. The minimum diameter for root detection using our experimental setup was 0.2 mm. The pixel size of 110–170 μm and background noise arising from soil heterogeneity prevented the detection of finer roots. Roots were detectable when there was at least a 10% difference in $\Sigma$ to the surrounding soil. At lower differences in $\Sigma$, measurement errors and background noise from soil heterogeneity prevented quantification.

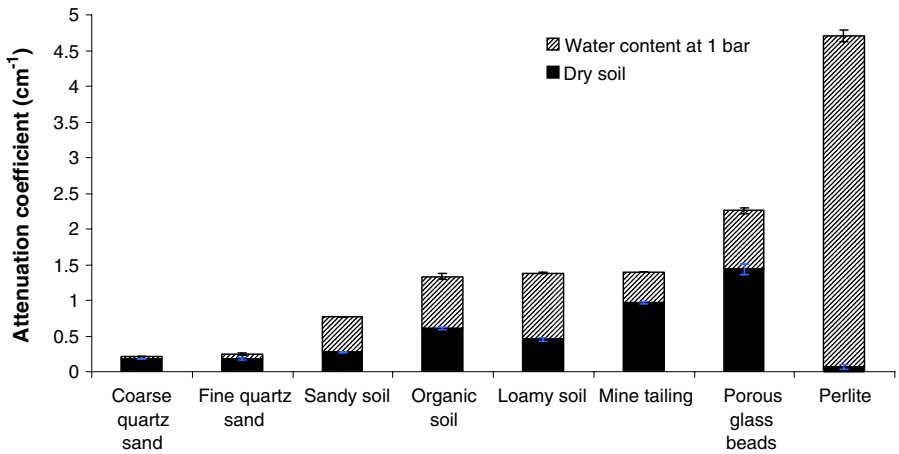


**Fig. 3** Cold-neutron attenuation coefficients of various root-growth materials, both dry and with a water content in equilibrium with −100 kPa

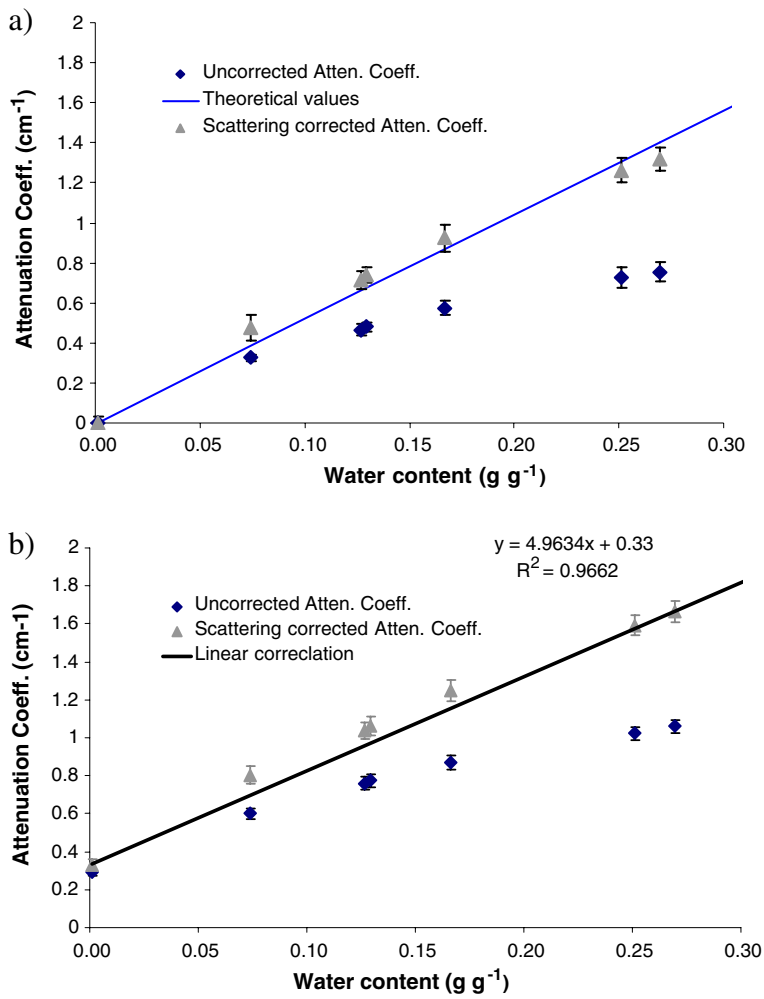


**Fig. 4** Scattering corrected and uncorrected cold-neutron attenuation coefficients of water in soil (**a**) and total water and soil materials (**b**) for a range of soil water contents. The scattering corrected and uncorrected attenuation coefficients are compared with the theoretical values. There is a linear correlation between the corrected attenuation coefficient and the soil water content (R2=0.966, Pearson confidence level >0.99). The error bars show standard deviation of the mean

At a soil $\theta$ below 0.1, the roots started dehydrating, which reduced contrast and inhibited plant growth. The flux of transmitted neutrons decreased at a soil $\theta$ above 0.25 due to high neutron scattering by soil water. This negatively affected the scattering correction and reduced contrast.

## Minimum detectable root diameter as a function of container thickness

Our container had an inner width of 12 mm in the direction of the neutron beam in order to provide enough space for the roots to grow. Others have used root-growth boxes that varied in thickness from 6 mm to more than 30 mm (Furukawa et al. 1999; Kuchenbuch and Ingram 2002; Nakanishi et al. 2003). Figure 5b shows how the minimum diameter of detectable roots depended on container thickness. This calculation was based on our results for the sandy soil using equations 3 and 4, assuming root $\theta$ of 85%, a soil $\theta$ of 0.12–0.18, a contrast threshold of 10% and no limitation in pixel size. With a container thickness of 4 mm, roots with a diameter of 0.04 mm could be resolved. The detectable root thickness increased exponentially with increasing the container width. With a container width of 25 mm, only roots thicker than 0.9 mm could be detected. The error bars show the variation in detectable root thickness over the range of optimal water contents for root imaging ($\theta$=0.12–0.18). As the container thickness increased, the error bars became smaller which means that the influence of soil $\theta$ on root detection decreased.

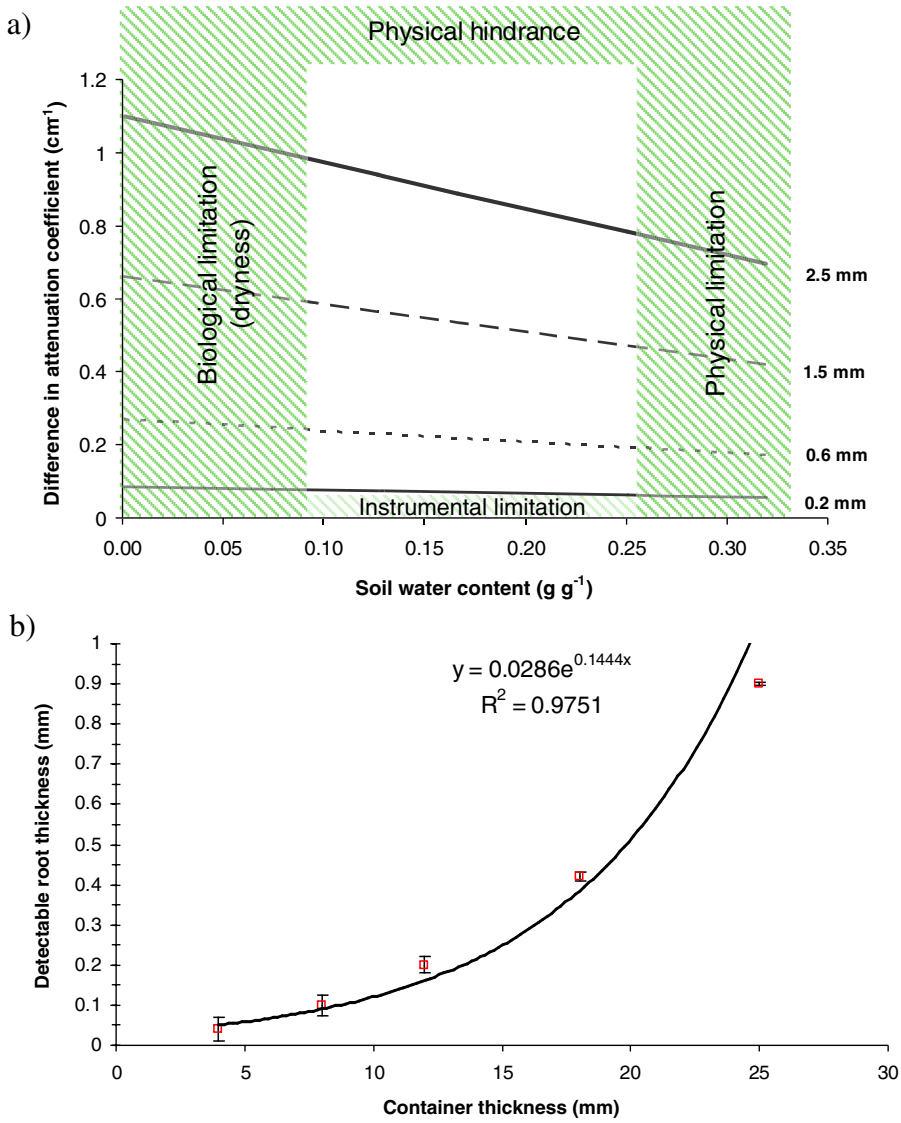


**Fig. 5** Calculated contrast in attenuation coefficient between roots of various thicknesses and surrounding soil as a function of soil water contents (**a**). The associated limitations are shown and minimum detectable root thicknesses are calculated for various container thicknesses (**b**). The error bars show the variation in detectable root thickness over the range of optimal water contents for root imaging ($\theta$=0.12–0.18)

NR, X-ray radiographs and scan photos of the plant roots

Figure 6 shows X-Ray, cold-neutron, and scan images of a 7 weeks old *Cicer arietinum* plant taken on the same day. Due to the weak contrast between soil and plant roots in the X-Ray image, (Fig. 6a), only major roots with a diameter of at least 1.5 mm could be seen. Roots had a lower X-Ray $\Sigma$ and appeared brighter than the surrounding soil because of their lower density and composition of light elements. Thus, most roots were veiled in the soil background. Neutron radiography provided a much higher contrast between the roots and the soil (Fig. 6b). The roots appeared darker than the surrounding soil in neutron radiograph due to their higher neutron attenuation coefficient than the soil. Not only main roots, but also lateral roots were also clearly visible. Figure 6c shows a scan of the soil surface after opening one side of the container. This method only showed roots on the surface and could not give a picture of roots enmeshed in the opaque soil.

The X-Ray and cold-neutron images of *Berkheya coddii* (Fig. 7a and b) had similar characteristics as the respective images of *Cicer arietinum*. Because *Berkheya coddii* also produces fine roots (<2 mm in diameter) in addition to the coarse main roots, the scan of the opened side of the soil (Fig. 7c) revealed

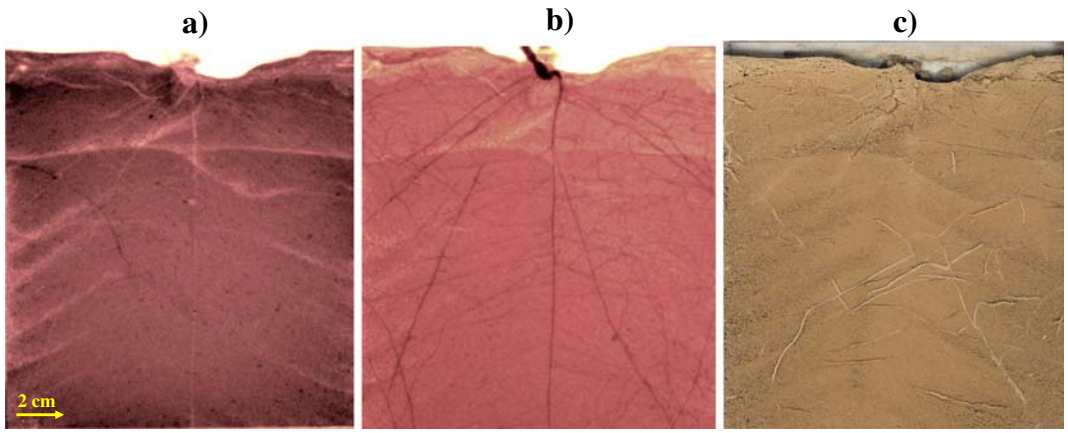


**Fig. 6** Comparison of X-Ray (**a**), cold-neutron (**b**), and scan (**c**) images of a 7 weeks old chickpea (*Cicer arietinum L.*) plant taken on the same day. While the X-Ray and scan image show only the main roots and the roots on the surface respectively, the neutron image reveals both fine roots and roots within the soil

many roots that were not visible in the neutron radiograph. The enlargement in Fig. 7c shows roots with thickness of 0.12 mm that could not be seen in the neutron radiograph because it was below the root-detection limit (0.2 mm). However, the root with thickness of 0.25 mm was clearly visible in both images.

*Lycopersicon esculentum* produces a fibrous rooting system of which most of the roots are in the range of 0.2 mm and thinner. Comparing the scanned image (Fig. 8c) with the neutron radiograph (Fig. 8b) revealed many fine roots that were only visible in the scanned image. These roots were mostly located at the bottom part of the container. In the X-Ray

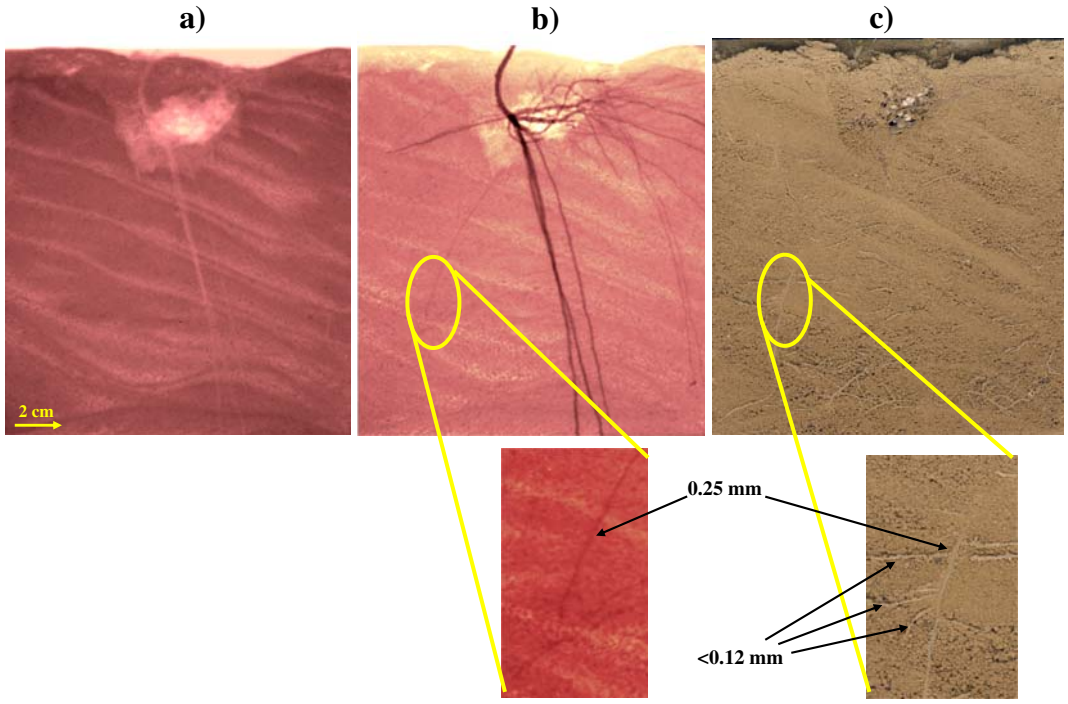


**Fig. 7** X-Ray (**a**), cold-neutron (**b**), and scan (**c**) images of a 7 weeks old *Berkheya coddii Roessl* plant. All the images were taken in the same day. Although the NR image reveals more roots than the other two techniques, but it fails to detect roots thinner than 0.2 mm, which are clearly visible in the scan image

radiograph (Fig. 8a) of this plant, no roots were visible except for the main root which had a thickness of more than 7 mm and was clearly visible.

## Discussions

### Root-soil contrast and choice of plant-growth medium

While soil contains typically less than 50% water by mass (in our case 20%), the $\theta$ of roots usually is in the range of 80–95%. Therefore, roots are best seen in soils with a low $\theta$, low intrinsic $\Sigma$ (meaning low concentrations of high neutron-absorbing elements), and low heterogeneity.

The choice of the plant growth medium is of overriding importance for root quantification with NR. An ideal plant growth medium for neutron imaging should provide enough contrast with roots, i.e. the lowest possible $\Sigma$, while providing a satisfactory environment for plant growth. The sandy soil (Fig. 3) was the best medium since it had a relatively low $\Sigma$ at both dry and wet conditions and still supported plant growth without water stress. Although fine and coarse quartz sands had lower $\Sigma$ than the sandy soil, mechanical resistance to root penetration due to high bulk density can be a problem for root growth (Menon et al. 2007).

### Correcting for scattering

Quantitative analysis of soil water and root distribution using NR requires scattering correction, especially when high concentrations of hydrogen are present in the system. Scattering had a large effect on radiographs taken within the range of soil $\theta$ that are optimum for root growth in most of the soils. Correcting for scattering improved the linearity between soil $\theta$ and the corresponding neutron attenuation coefficients (Fig. 4). Such linearity greatly enhances the reliability and sensitivity (up to 80%) of the calibration curve and simplifies the use of the calibration curve for relating water content to the attenuation coefficient which is crucial for quantitative analysis of roots and water distribution in soil by means of NR.

### NR in relation to X-ray and scan photos

NR revealed the details of the roots the most among the other two methods (Figs. 6, 7 and 8). X-ray radiographs had a weaker contrast between the roots and the soil than NR. Using microfocus X-Ray sources could improve the spatial resolution and the contrast between roots and the surrounding soil. Although our X-Ray imaging system had a large focal spot, (3 mm), it provided detailed information on the soil structure: textural layers created by the filling process and the cracks in the soil were clearly

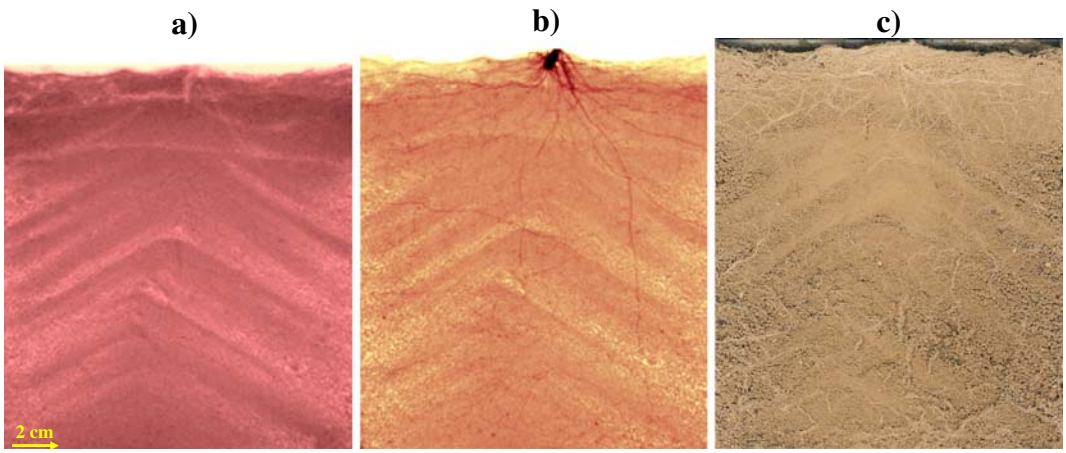


**Fig. 8** Comparison of X-Ray (**a**), cold-neutron (**b**), and scan (**c**) images of a 7 weeks old tomato (*Lycopersicon sculentum Mill*) taken on the same day. No roots are visible in the X-Ray image and the neutron image fails to reveal the fine roots especially in the bottom of the container (which is clearly visible in the scan image) although it reveals the thicker roots in the upper part of the container

visible. Therefore, X-Ray and neutron images provide complementary information on the root-soil system. X-Ray radiography, which provides information on soil texture, could be used to enhance root contrast by revealing the position of non-root features in the rhizosphere.

Scan images provided details of the roots only on the soil surface. Scan images could be useful to estimate the proportion of roots with a diameter of <2 mm, which were not detectable using NR. These very fine roots are mostly lost when roots are physically separated from soil.

## Advantages and limitations of NR for the visualisation of plant roots

With respect to quantitative root system analysis, NR application is currently still limited at high soil $\theta$ due to high neutron scattering, and at low soil $\theta$, due to root dehydration (Fig. 5a). Improvements in instrumentation, in particular, higher resolution detector systems, will permit the visualisation of roots with a diameter of <0.2 mm. Nevertheless, NR currently can image roots with a thickness of ≥0.2 mm and in a range of soil $\theta$ (0.1–0.25) that is well suited for plant growth. Using thermal neutrons with higher energy and, therefore higher penetration, permits the visualisation of root growth at soil $\theta$>0.25 (data not shown), although the contrast is reduced.

**Acknowledgements** This study was funded by the Swiss National Science Foundation. Dr. Héctor Conesa had a grant from Fundación Séneca of Comunidad Autónoma de Murcia (Spain).

## References

Allen RG, Pererira LS, Raes D, Smith M (1998) Crop evapotranspiration. Guidelines for computing crop water requirements. FAO, Rome

Bailey IF (2003) A review of sample environments in neutron scattering. Zeitschrift Fur Kristallographie 218:84–95

Bois JF, Couchat P (1983) Comparison of the effects of water-stress on the root systems of 2 cultivars of upland rice (Oryza-Sativa-L). Ann Bot 52:479–487

Bottomley PA, Rogers HH, Prior SA (1993) Nmr imaging of root water distribution in intact Vicia-Faba L plants in elevated atmospheric Co2. Plant Cell Environ 16:335–338

Costa C, Dwyer LM, Hamel C, Muamba DF, Wang XL, Nantais L, Smith DL (2001) Root contrast enhancement for measurement with optical scanner-based image analysis. Can J Bot-Revue Canadienne De Botanique 79:23–29

Doussan C, Pages L, Pierret A (2003) Soil exploration and resource acquisition by plant roots: an architectural and modelling point of view. Agronomie 23:419–431

Fitz W, Puschenreiter M, Schweiger P, Wenzel WW (2005) Novel tools for investigating rhizosphere processes. Abstracts of Papers of the American Chemical Society 230:U1789–U1790

Furukawa J, Nakanishi TM, Matsubayashi H (1999) Neutron radiography of a root growing in soil with vanadium. Nucl Instrum Methods Phys Res Sect A 424:116–121

Gregory PJ, Hutchison DJ, Read DB, Jenneson PM, Gilboy WB, Morton EJ (2003) Non-invasive imaging of roots with high resolution X-ray micro-tomography. Plant Soil 255:351–359

Hall LD, Amin MHG, Dougherty E, Sanda M, Votrubova J, Richards KS, Chorley RJ, Cislerova M (1997) MR properties of water in saturated soils and resulting loss of MRI signal in water content detection at 2 tesla. Geoderma 80:431–448

Hassanein RK (2006) Correction methods for the quantitative evaluation of thermal neutron tomography. ETH Zurich, Switzerland

Hassanein R, Lehmann E, Vontobel P (2005) Methods of scattering corrections for quantitative neutron radiography. Nucl Instrum Methods Phys Res Sect A 542:353–360

Heyes JA, Clark CJ (2003) Magnetic resonance imaging of water movement through asparagus. Funct Plant Biol 30:1089–1095

Hoagland DR, Arnon DI (1938) The water culture method for growing plants without soil. Calif Agric Exp Stn 347:1–39

Kasperl S, Vontobel P (2005) Application of an iterative artefact reduction method to neutron tomography. Nucl Instrum Methods Phys Res Sect A 542:392–398

Kuchenbuch RO, Ingram KT (2002) Image analysis for non-destructive and non-invasive quantification of root growth and soil water content in rhizotrons. Journal of Plant Nutrition and Soil Science-Z PflanzenernaÉhr Bodenkd 165:573–581

Kuhne G, Frei G, Lehmann E, Vontobel P (2005) CNR—the new beamline for cold neutron imaging at the Swiss spallation neutron source SINQ. Nucl Instrum Methods Phys Res Sect A 542:264–270

Lehmann E, Pleinert H, Williams T, Pralong C (1999) Application of new radiation detection techniques at the Paul Scherrer Institut, especially at the spallation neutron source. Nucl Instrum Methods Phys Res Sect A 424:158–164

Majdi H (1996) Root sampling methods—Applications and limitations of the minirhizotron technique. Plant Soil 185:255–258

Matsushima U, Kawabata Y, Hino M, Geltenbort P, Nicolai BM (2005) Measurement of changes in water thickness in plant materials using very low-energy neutron radiography. Nucl Instrum Methods Phys Res Sect A 542:76–80

Menon M, Robinson B, Oswald SE, Kaestner A, Abbaspour KC, Lehmann E, Schulin R (2007) Visualization of root growth in heterogeneously contaminated soil using neutron radiography. Eur J Soil Sci 58:802–810

Moran CJ, Pierret A, Stevenson AW (2000) X-ray absorption and phase contrast imaging to study the interplay between plant roots and soil structure. Plant Soil 223:99–115

Naftel SJ, Martin RR, Sham TK, Macfie SM, Jones KW (2001) Micro-synchrotron X-ray fluorescence of cadmium-challenged corn roots. J Electron Spectrosc Relat Phenom 119:235–239

Nakaji T, Noguchi K, Oguma H (2008) Classification of rhizosphere components using visible-near infrared spectral images. Plant Soil 310:245–261

Nakanishi TM, Okuni Y, Furukawa J, Tanoi K, Yokota H, Ikeue N, Matsubayashi M, Uchida H, Tsiji A (2003) Water movement in a plant sample by neutron beam analysis as well as positron emission tracer imaging system. J Radioanal Nucl Chem 255:149–153

Nakanishi TM, Okuni Y, Hayashi Y, Nishiyama H (2005) Water gradient profiles at bean plant roots determined by neutron beam analysis. J Radioanal Nucl Chem 264:313–317

Oswald SE, Menon M, Robinson B, Carminati A, Vontobel P, Lehmann E, Schulin R (2008) Quantitative imaging of infiltration, root growth, and root water uptake via neutron radiography. Vadose Zone Journal 7:1035–1047

Pierret A (2008) Multi-spectral imaging of rhizobox systems: new perspectives for the observation and discrimination of rhizosphere components. Plant Soil 310:263–268

Pierret A, Doussan C, Garrigues E, Mc Kirby J (2003a) Observing plant roots in their environment: current imaging options and specific contribution of two-dimensional approaches. Agronomie 23:471–479

Pierret A, Kirby M, Moran C (2003b) Simultaneous X-ray imaging of plant root growth and water uptake in thin-slab systems. Plant Soil 255:361–373

Pierret A, Moran CJ, Doussan C (2005) Conventional detection methodology is limiting our ability to understand the roles and functions of fine roots. New Phytol 166:967–980

Sutton RF, Tinus RW (1983) Root and root system terminology. For Sci Monogr 24:137

Tumlinson LG, Liu HY, Silk WK, Hopmans JW (2008) Thermal neutron computed tomography of soil water and plant roots. Soil Sci Soc Am J 72:1234–1242

Vogt KA, Vogt DJ, Bloomfield J (1998) Analysis of some direct and indirect methods for estimating root biomass and production of forests at an ecosystem level. Plant Soil 200:71–89

Waisel Y, Eshel A, Kafkafi Z (Eds.) (2002) Plant roots: the hidden half. Marcel Dekker, New York

Willatt ST, Struss RG (1979) Germination and early growth of plants studied using neutron radiography. Ann Bot 43:415–422

Willatt ST, Struss RG, Taylor HM (1978) Insitu root studies using neutron radiography. Agron J 70:581–586